

AUTHOR QUERY FORM**Journal:** DEVCEL**Article Number:** 3668

Dear Author,

Please check your proof carefully and mark all corrections at the appropriate place in the proof.

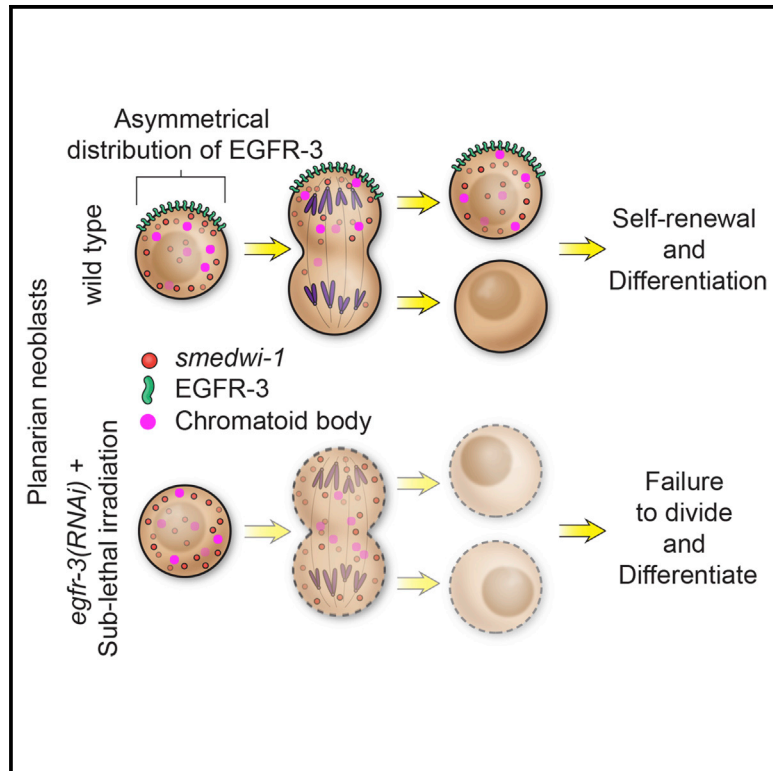
Location in article	Query / Remark: Click on the Q link to find the query's location in text Please insert your reply or correction at the corresponding line in the proof
Q1	Cell Press policy requires that all papers include a "Lead Contact" designation. The lead contact functions as the lead communication contact for the journal, the primary contact for reagent and resource sharing, and the arbiter of decisions and disputes. Could you please let me know which corresponding author should be designated as the lead contact?
Q2	Please explain what the asterisks indicate in part I of Figure 1, in its corresponding figure legend.

Thank you for your assistance.

Developmental Cell

Egf Signaling Directs Neoblast Repopulation by Regulating Asymmetric Cell Division in Planarians

Graphical Abstract



Authors

Kai Lei, Hanh Thi-Kim Vu,
 Ryan D. Mohan, ..., Kirsten Gotting,
 Jerry L. Workman,
 Alejandro Sánchez Alvarado

Correspondence

kle@stowers.org (K.L.),
 asa@stowers.org (A.S.A.)

In Brief

Stem cell repopulation can be achieved from even a single pluripotent stem cell in planarian flatworms. Lei et al. show that EGF signaling is required for stem cell repopulation in *Schmidtea mediterranea*, which is regulated through proper control of symmetric versus asymmetric cell division.

Highlights

- *egfr-3* is required for neoblast repopulation after sublethal irradiation
- The putative EGF ligand *neuregulin-7* also regulates neoblast repopulation
- *Ikb1*, *ampk*, and *rad54B* function downstream of *egfr-3* during neoblast repopulation
- *egfr-3* regulates asymmetric cell division in neoblast repopulation

Accession Numbers

GSE84025

Egf Signaling Directs Neoblast Repopulation by Regulating Asymmetric Cell Division in Planarians

Q1 Kai Lei,^{1,*} Hanh Thi-Kim Vu,¹ Ryan D. Mohan,² Sean A. McKinney,¹ Chris W. Seidel,¹ Richard Alexander,¹ Kirsten Gotting,¹ Jerry L. Workman,¹ and Alejandro Sánchez Alvarado^{1,3,*}

¹Stowers Institute for Medical Research, Kansas City, MO 64110, USA

²Division of Cell Biology and Biophysics, School of Biological Sciences, University of Missouri-Kansas City, Kansas City, MO 64110, USA

³Howard Hughes Medical Institute, Stowers Institute for Medical Research, Kansas City, MO 64110, USA

*Correspondence: kle@stowers.org (K.L.), asa@stowers.org (A.S.A.)

<http://dx.doi.org/10.1016/j.devcel.2016.07.012>

SUMMARY

A large population of proliferative stem cells (neoblasts) is required for physiological tissue homeostasis and post-injury regeneration in planarians. Recent studies indicate that survival of a few neoblasts after sublethal irradiation results in the clonal expansion of the surviving stem cells and the eventual restoration of tissue homeostasis and regenerative capacity. However, the precise mechanisms regulating the population dynamics of neoblasts remain largely unknown. Here, we uncovered a central role for epidermal growth factor (EGF) signaling during *in vivo* neoblast expansion mediated by *Smed-egfr-3* (*egfr-3*) and its putative ligand *Smed-neuregulin-7* (*nrg-7*). Furthermore, the EGF receptor-3 protein localizes asymmetrically on the cytoplasmic membrane of neoblasts, and the ratio of asymmetric to symmetric cell divisions decreases significantly in *egfr-3*(*RNAi*) worms. Our results not only provide the first molecular evidence of asymmetric stem cell divisions in planarians, but they also demonstrate that EGF signaling likely functions as an essential regulator of neoblast clonal expansion.

INTRODUCTION

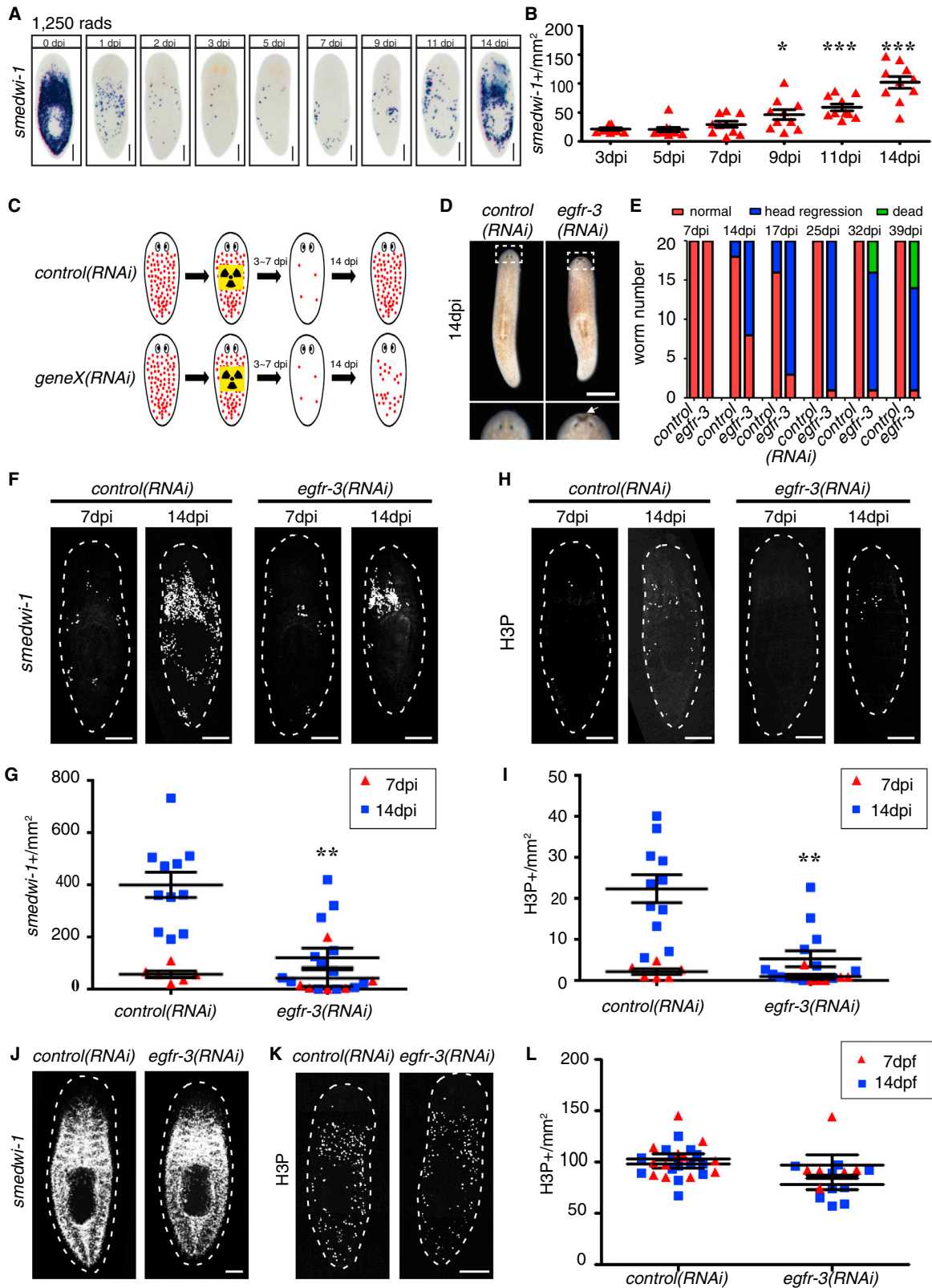
The ability of planarians to restore their stem cells after substantial damage is in contrast to mammals, which lack a robust capacity to replenish a variety of stem cell pools after ablation by chemo- or radiotherapy (Biteau et al., 2011; Miyajima et al., 2014; Vermeulen and Snippert, 2014). Self-renewal and the production of differentiated progeny are key stem cell attributes required to sustain the function of many adult tissues (Hsu and Fuchs, 2012). Understanding how planarian stem cells regulate these processes during homeostasis and in response to injury has important implications for regenerative medicine and for developing effective cancer therapies.

Planarians harbor a remarkable capacity to regenerate complete animals from small tissue fragments (Morgan, 1900; Sán-

chez Alvarado and Newmark, 1998). This ability derives, in part, from an abundant population of adult stem cells collectively known as neoblasts (Baguña et al., 1989a, 1989b; Reddien and Sánchez Alvarado, 2004). In asexually reproducing planarians, neoblasts are the only known proliferating cells (Newmark and Sánchez Alvarado, 2000). As such, it is possible to completely or partially ablate these cells by exposing animals to ionizing radiation (Bardeen and Baetjer, 1904; Guedelhoefer and Sánchez Alvarado, 2012; Reddien et al., 2005; Reddien and Sánchez Alvarado, 2004; Wolff and Dubois, 1948). Interestingly, these two experimental paradigms have helped demonstrate that the entire population of planarian stem cells can be fully reconstituted from a single pluripotent neoblast presently termed “cNeoblast” (Salveti et al., 2009; Wagner et al., 2011, 2012). Therefore, the robust stem cell regulation occurring in planarians combined with methodologies to effectively visualize neoblasts at whole-organism resolution makes these animals a powerful *in vivo* model system to study the molecular mechanisms underpinning adult stem cell repopulation and the dynamics of stem cell populations under normal and aberrant conditions.

Extracellular signals usually associated with stem cell niches such as epidermal growth factor (EGF), fibroblast growth factor (FGF), vascular endothelial growth factor (VEGF), Wnt, Notch, and transforming growth factor β (TGF- β) are known to play prominent roles in regulating stem cell homeostasis and repopulation in vertebrate and invertebrate species (Hogan et al., 2014; Hsu and Fuchs, 2012; Kotton and Morrisey, 2014; Mendelson and Frenette, 2014; Shi and Garry, 2006). In many organisms, these extracellular signals affect cell proliferation by regulating the frequency of cell division (Alberts et al., 2002) and/or the type of daughter cells produced by modulating whether symmetric or asymmetric cell divisions take place (Morrison and Kimble, 2006; Neumuller and Knoblich, 2009). However, the roles that developmental signaling pathways play in neoblast population dynamics remain unclear.

In planarians, it is known that Wnt/ β -catenin and Hedgehog signaling are required for establishing anterior-posterior polarity during homeostasis and tissue regeneration (Adell et al., 2009; Gurley et al., 2008; Iglesias et al., 2008; Kobayashi et al., 2007; Petersen and Reddien, 2008, 2009; Reddien et al., 2007; Rink et al., 2009). TGF- β signaling is essential for maintenance and regeneration of dorsal-ventral and medial-lateral axes (Gaviño



(legend on next page)

and Reddien, 2011; Molina et al., 2007; Reddien et al., 2007), as well as for sensing signals related to wound and/or missing tissues (Gaviño et al., 2013; Roberts-Galbraith and Newmark, 2013; Yazawa et al., 2009). FGF signaling is required for brain patterning (Cebrià et al., 2002) and tissue homeostasis (Wagner et al., 2012). EGF and insulin signaling pathways are crucial for maintenance of the neoblast population during homeostasis and regeneration (Fraguas et al., 2011; Miller and Newmark, 2012). However, little is known about the potential functions these signaling pathways may play in regulating neoblast population dynamics, and no roles have been reported for any of these pathways in modulating neoblast repopulation after challenge by sublethal irradiation. For example, a previous RNAi screen aimed at identifying modulators of stem cell proliferation and differentiation did not include these pathways except for FGF (Wagner et al., 2012). In addition, even though both symmetric and asymmetric cell divisions within the planarian stem cell pool have long been hypothesized to occur, no direct evidence demonstrating these two phenomena has yet been put forward (Coward, 1974; Reddien, 2013; Rink, 2013; Zhu et al., 2015).

In this study, we aimed to determine whether the EGF, FGF, insulin, VEGF, TGF- β , Wnt/ β -catenin, Hedgehog, and/or Notch signaling pathways play a role in regulating the proliferation dynamics of planarian stem cells. By taking advantage of double-stranded RNA (dsRNA)-mediated gene knockdown (Newmark et al., 2003; Reddien et al., 2005) and a colony expansion assay (Wagner et al., 2012), we performed a screen to test whether abrogation of signaling pathways would have an effect on neoblast expansion after sublethal irradiation. We found that EGF receptor 3 (EGFR-3) and a putative planarian EGF ligand, NEUREGULIN-7, are required for neoblast repopulation. In addition, a candidate approach and RNA-sequencing (RNA-seq) analysis revealed EGFR-3 downstream factors, including *lkb1*, *ampk*, and a DNA-damage response gene *rad54b*, as being required for neoblast repopulation following sublethal irradiation. We also provide evidence for the existence of asymmetric cell division in planarian stem cells and show that asymmetric cell division and early progeny differentiation during neoblast repopulation is blocked in *egfr-3(RNAi)* worms. We propose that EGF signaling plays a central role in regulating asymmetric cell division and cell-fate decision during neoblast repopulation.

RESULTS

egfr-3 Is Required for Neoblast Repopulation after Sublethal Irradiation

To assess the role of evolutionarily conserved extracellular signaling pathways in regulating stem cell repopulation, we first determined which of these candidate genes were expressed in neoblasts. Since neoblasts can be selectively eliminated within 24 hr following lethal irradiation (Reddien et al., 2005), we compared the expression of candidate genes in normal versus lethally irradiated planarians. We performed whole-mount in situ hybridization (WISH) for the receptors of EGF (*egfr-1*, *egfr-2*, *egfr-3*), FGF (*fgfr-1*, *fgfr-2*, *fgfr-3*, *fgfr-4*), TGF- β (*activinR-1*, *activinR-2*), insulin (*inr-1*), VEGF (*vegfr-1*), and Hedgehog (*ptc*) pathways. We also assessed the expression of the transcriptional effectors of the canonical Wnt (β -*catenin-1*) and Notch (*su(H)*) pathways. After lethal irradiation (6,000 rad) and 1 day post irradiation (dpi), we detected a noticeable decrease in the expression levels of *egfr-3*, *fgfr-1*, *fgfr-3*, *fgfr-4*, and *inr-1* (Figure S1A), suggesting expression of these genes in neoblasts. We then carried out double fluorescence in situ hybridization (FISH) with the neoblast-specific marker *smedwi-1* to examine *egfr-3*, *fgfr-1*, *fgfr-3*, *fgfr-4*, and *inr-1* co-expression. Indeed, the majority of the *egfr-3*⁺ (85%), *fgfr-1*⁺ (79%), *fgfr-3*⁺ (74%), *fgfr-4*⁺ (92%), and *inr-1*⁺ (100%) cells also expressed *smedwi-1* (Figure S1B), consistent with previous reports (Fraguas et al., 2011; Miller and Newmark, 2012; Ogawa et al., 2002; Wagner et al., 2012). This suggests a functional role for the EGF, FGF, and insulin pathways in neoblasts.

Next, we confirmed previous observations on the dynamics of neoblast repopulation following sublethal (1,250 rad) irradiation (Wagner et al., 2011, 2012), and defined a quantitative neoblast depletion and recovery assay that scores *smedwi-1*⁺ cells at 0, 1, 2, 3, 5, 7, 9, 11, and 14 dpi. We noted the total number of neoblasts decreased dramatically within the first 3 days (Figure 1A), followed by a significant increase at 7 dpi in control animals (Figures 1A and 1B, 14 dpi). To determine whether the candidate EGF, FGF, or insulin receptors are required for neoblast repopulation, we reasoned that the number of neoblasts in both control and RNAi-treated animals should be comparable at 7 dpi, but significantly lower in RNAi-treated animals at 14 dpi (Figure 1C). Using this assay, we quantified the density of neoblasts in control versus RNAi-treated planarians at 7 and 14 dpi (Figure 1C).

Figure 1. *egfr-3* Is Required for Neoblast Repopulation

- (A) *smedwi-1* WISH of uninjured wild-type planarians exposed to sublethal irradiation (1,250 rad) at indicated days post irradiation (dpi).
 (B) Quantification of *smedwi-1*⁺ cells/mm² following sublethal irradiation in wild-type planarians. Each triangle represents one animal. Error bars denote SEM. *p < 0.05, ***p < 0.001 compared with 3 dpi.
 (C) Experimental strategy to identify gene(s) (geneX) required for neoblast repopulation following sublethal irradiation. Red dots represent *smedwi-1*⁺ neoblasts.
 (D) Live *egfr-3(RNAi)* planarians display head regression at 14 dpi following 1,250 rad of irradiation. The dashed boxes and arrows indicate the area with head regression in *egfr-3(RNAi)* but not in control animals.
 (E) Histogram of number of *control(RNAi)* versus *egfr-3(RNAi)* planarians with head regression or death at indicated times.
 (F) *control(RNAi)* and *egfr-3(RNAi)* planarians at 7 and 14 dpi stained for *smedwi-1* FISH.
 (G) Quantification of *smedwi-1*⁺ cells/mm² in *egfr-3(RNAi)* planarians. **p < 0.01 versus *control(RNAi)*.
 (H) *control(RNAi)* and *egfr-3(RNAi)* planarians at 7 and 14 dpi immunostained with anti-H3P antibody.
 (I) Quantification of H3P⁺ cells/mm² in sublethally irradiated *egfr-3(RNAi)* planarians.
 (J) Unirradiated *control(RNAi)* and *egfr-3(RNAi)* planarians stained for *smedwi-1* FISH.
 (K) Unirradiated *control(RNAi)* and *egfr-3(RNAi)* planarians immunostained with anti-H3P antibody.
 (L) Quantification of H3P⁺ cells/mm² in unirradiated *egfr-3(RNAi)* planarians compared with controls.
 Scale bars represent 200 μ m (A, D) and 500 μ m (F, H, J, K). See also Figures S1 and S2.

Q2

Neither individual, nor combination knockdown of *fgfr-1*, *fgfr-3*, or *fgfr-4* caused defects in neoblast repopulation after sublethal irradiation (Figures S1C–S1F). On the other hand, *inr-1(RNAi)* ablated the neoblast population in both unirradiated and sublethally irradiated planarians, and caused locomotion defects (Figures S2A–S2E and S2K–S2M). When assayed by *smcdwi-1* FISH and immunostaining for mitotic cells using an anti-phospho-histone H3 (Ser10) antibody (anti-H3P), RNAi of *insulin-like peptide 1 (ilp-1)* (Figure S2F) (Miller and Newmark, 2012) yielded similar numbers of *smcdwi-1*⁺ and H3P⁺ cells in unirradiated planarians compared with controls (Figures S2K–S2M), while in sublethal irradiations it resulted in slower neoblast repopulation (Figures S2G–S2J). In marked contrast, *egfr-3(RNAi)* animals displayed a density of neoblasts and mitotic cells similar to that of controls at 7 dpi, but significantly lower at 14 dpi (Figures 1F–1I). *egfr-3(RNAi)* planarians also showed head regression after 14 dpi and ultimately lysed, while *control(RNAi)* animals recovered (Figures 1D and 1E). Consistent with a previous report (Fraguas et al., 2011), no significant change in *smcdwi-1*⁺ and H3P⁺ cell density was observed in unirradiated *egfr-3(RNAi)* planarians (Figures 1J–1L). Flow cytometry analyses further confirmed that neoblasts did not decrease in number before sublethal irradiation in *egfr-3(RNAi)* planarians (Figure S1G).

Altogether, these data indicate that FGF signaling may not be required for neoblast repopulation. In contrast, insulin signaling facilitates both homeostatic neoblast population maintenance and expansion after irradiation damage, and additional insulin-like peptides may exist and function redundantly with *ilp-1*. Only *egfr-3(RNAi)* specifically prevented neoblast expansion without affecting homeostasis. We conclude that EGF signaling via *egfr-3* is required for the expansion of neoblasts when their numbers are diminished by sublethal irradiation and that this role is distinct from that of other signaling molecules.

***egfr-3* Is Required for Cell Proliferation during Neoblast Repopulation**

Defects in neoblast repopulation can be caused by either slower proliferation or increased cell death. To distinguish between these two possibilities, we carried out BrdU labeling and TUNEL assays, respectively. Cells were labeled with BrdU for 4 hr in *control(RNAi)* and *egfr-3(RNAi)* at 7 dpi (Figure 2A). In controls, the number of BrdU⁺ cells increased gradually and doubled approximately 24 hr after labeling (Figures 2B and 2D). However, no obvious increase was observed in *egfr-3(RNAi)* (Figures 2C and 2D). Furthermore, *smcdwi-1*⁺ cells increased in *control(RNAi)*, but not in *egfr-3(RNAi)* (Figures 2E–2G). These results suggest that *egfr-3* promotes cell proliferation during neoblast repopulation.

To examine apoptosis, we carried out TUNEL assays in *control(RNAi)* and *egfr-3(RNAi)* animals after sublethal irradiation. In controls there was a large number of apoptotic cells at 1 dpi, which was consistent with the observed neoblast depletion during this time (Figures 2H and 2I). After 3 dpi, the density of TUNEL⁺ cells leveled off in controls (Figures 2H and 2I). In *egfr-3(RNAi)* animals, the density of TUNEL⁺ cells was similar to that of controls at 13 dpi (Figures 2J and 2K), suggesting that *egfr-3* may not drastically affect the extent of apoptosis during neoblast repopulation. Therefore, the *egfr-3(RNAi)* repo-

pulation defects appear likely to be due to a failure in neoblast proliferation following sublethal irradiation.

Previous studies have shown that amputation induces neoblast proliferation (Newmark and Sánchez Alvarado, 2000; Wenemoser and Reddien, 2010). We therefore tested whether *egfr-3* also functions in amputation-induced cell proliferation. *Control(RNAi)* and *egfr-3(RNAi)* planarians were amputated and immunostained with anti-H3P antibody to compare the number of proliferating cells. Consistent with a previous report (Fraguas et al., 2011), *egfr-3(RNAi)* animals displayed impaired regeneration at 3 days post amputation (Figure S3A). At 6 hr post amputation (hpa), the first peak of amputation-induced hyperproliferation was slightly lower in *egfr-3(RNAi)* compared with controls (Figures S3B and S3C). In contrast, the second peak of hyperproliferation at 48 hpa was dramatically decreased in *egfr-3(RNAi)* animals (Figures S3B and S3C). These results suggest that *egfr-3* is required for both phases of regeneration-associated hyperproliferation.

The Putative EGF Ligand *Neuregulin-7* Also Regulates Neoblast Repopulation

Since *egfr-3* is a signaling molecule that appears to play a significant role in neoblast repopulation, we sought to identify its upstream ligands. Twelve putative EGF ligands were predicted to exist in the planarian genome based upon EGF domain and homology sequence comparisons (Figures S4A and S4B). Their expression patterns were examined by WISH in unirradiated and lethally irradiated planarians (6,000 rad, 1 dpi) (Figure 3A). None of the tested ligand-encoding genes were expressed in irradiation-sensitive cells, suggesting that they do not show enriched expression in neoblasts. To examine their function in neoblast repopulation, we screened the putative ligands in the sublethal irradiation assay following RNAi feeding (see Figure 1C for experimental strategy) and found that only *neuregulin-7 (nrg-7)* RNAi robustly impaired neoblast repopulation (Figures 3B–3E and S4C–S4I). Like *egfr-3(RNAi)*, *nrg-7(RNAi)* did not affect the homeostasis of the neoblast population compared with controls (Figures 3F–3H), nor did it affect regeneration. As was the case in *egfr-3(RNAi)* animals, flow cytometry analyses further confirmed that neoblasts did not decrease in number before sublethal irradiation in *nrg-7(RNAi)* planarians (Figure S4J), nor was recovery observed. To determine the cell types in which *nrg-7* is expressed, we performed *nrg-7* FISH with *smcdwi-1*, epidermal progeny markers (early and late progeny *prog-1* and *agat*), and differentiated cell markers (muscle: *collagen*; CNS: *PC2*). We found that *nrg-7* was expressed in *prog-1*⁺ and *PC2*⁺ cells (Figure S4K). To test whether this molecule could interact with EGFR-3, we performed in vitro binding assays using purified recombinant EGFR-3 and NRG-7. Our analyses showed a direct interaction between NRG-7 and EGFR-3 in vitro (Figure 3I). Together, these data suggest that NRG-7 is a likely ligand of EGFR-3 required during neoblast repopulation.

***lkb1* and *ampk* Function Downstream of *egfr-3* during Neoblast Repopulation**

To better understand how *egfr-3* regulates neoblast repopulation, we tested the function of downstream, conserved EGF pathway components *erk*, *pi3k*, *stat*, *lkb1*, and *ampk*. First, WISH was performed to examine their respective expression

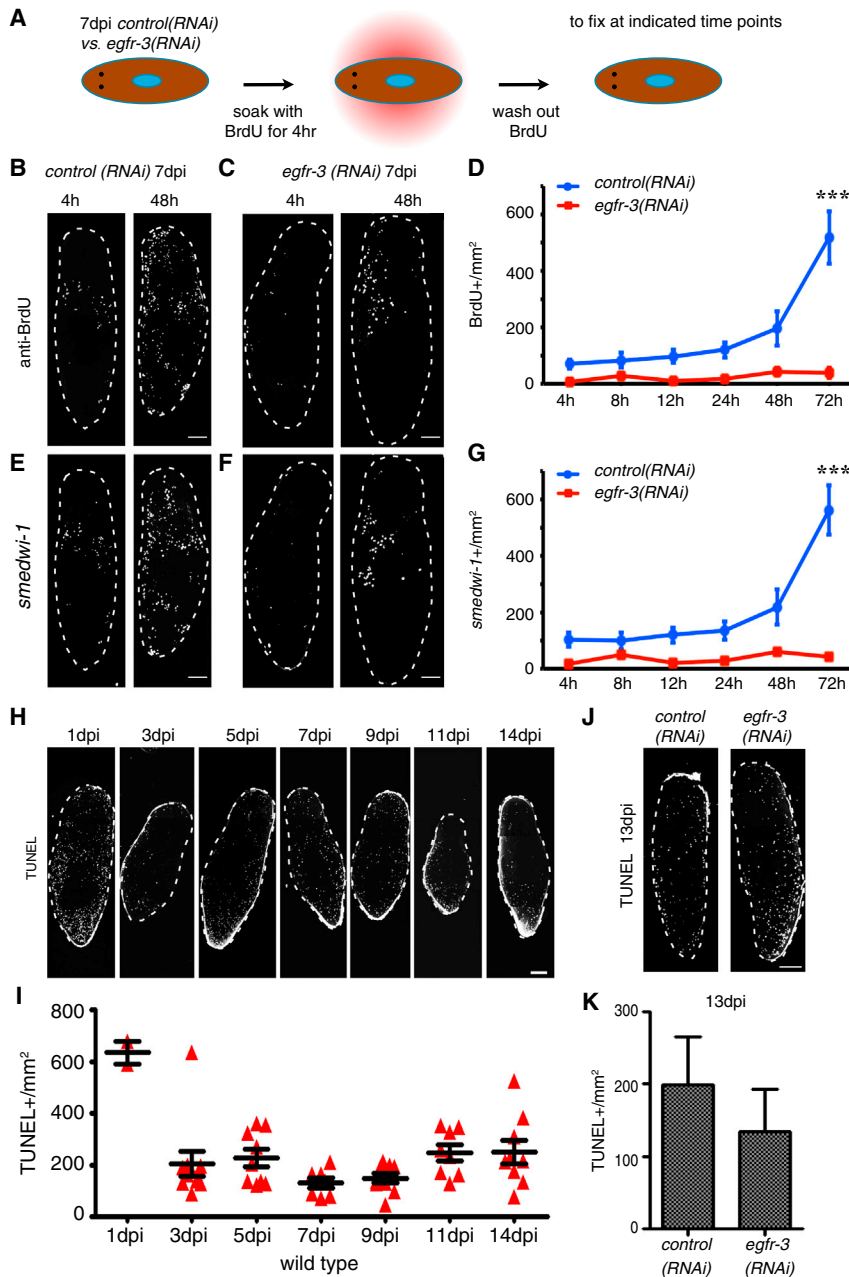


Figure 2. *egfr-3(RNAi)* Affects Cell Proliferation but Not Cell Apoptosis during Neoblast Repopulation

(A) Strategy for comparing cell proliferation in *control(RNAi)* and *egfr-3(RNAi)* animals at 7 dpi via BrdU pulse-chase.

(B and C) BrdU⁺ cells in *control(RNAi)* (B) and *egfr-3(RNAi)* (C) planarians at 4 and 48 hr after BrdU soaking. h, hour. Scale bars, 200 μ m.

(D) Quantification of BrdU⁺ cells/mm² in *egfr-3(RNAi)* planarians versus controls at 72 hr post chase. ****p* < 0.001.

(E and F) FISH for *smedwi-1* shows neoblasts in *control(RNAi)* (E) and *egfr-3(RNAi)* (F) planarians at 4 and 48 hr after BrdU labeling. Scale bars, 200 μ m.

(G) Quantification of *smedwi-1*⁺ cells/mm² in *egfr-3(RNAi)* planarians compared with controls at 72 hr post chase. ****p* < 0.001.

(H) TUNEL-positive nuclei of cells in wild-type planarians at indicated time points after irradiation with 1,250 rad. Scale bar, 200 μ m.

(I) Quantification of TUNEL⁺ nuclei/mm² at indicated time points after 1,250 rad of irradiation.

(J) TUNEL staining of apoptotic cells in *control(RNAi)* and *egfr-3(RNAi)* planarians at 13 dpi. Scale bars, 500 μ m.

(K) Quantification of TUNEL⁺ nuclei/mm² in *control(RNAi)* and *egfr-3(RNAi)* planarians at 13 dpi.

See also Figure S3.

results suggest that *egfr-3* regulates neoblast repopulation through the *lkb1-ampk* branch of the EGF signaling pathway; however, future biochemical work assessing pathway activation is still needed.

rad54b Is Likely an Effector of *egfr-3* Signaling in Neoblast Repopulation

To further address how *egfr-3* may regulate changes in gene expression during neoblast repopulation, we used an RNA-seq approach to identify differentially expressed genes in *control(RNAi)* versus *egfr-3(RNAi)* planarians in whole animals during neoblast repopulation and in isolated neoblasts (X1 cells) from unirradiated animals (Figure 5A). During neoblast re-

population in wild-type and lethally irradiated animals (6,000 rad, 1 dpi). While none of these genes displayed obvious neoblast expression patterns, *erk-1*, *lkb1*, and *ampk* were noticeably decreased after 6,000 rad (Figures 4A, S5A, and S5B). Double FISH with *smedwi-1* confirmed that *erk-1*, *lkb1*, and *ampk* were expressed in neoblasts (Figures 4B and S5C). To determine whether any of these downstream effectors were required for neoblast repopulation, we subjected RNAi-treated animals to sublethal irradiation (1,250 rad). *erk-1(RNAi)* planarians displayed normal neoblast repopulation (Figures S5D–S5G). However, *lkb1(RNAi)* and *ampk(RNAi)* showed disrupted neoblast repopulation (Figures 4C–4F). Similar to *egfr-3(RNAi)*, unirradiated *lkb1(RNAi)* and *ampk(RNAi)* planarians maintained normal levels of neoblasts and proliferating cells (Figures 4G–4I). These

patterns in wild-type and lethally irradiated animals (6,000 rad, 1 dpi). While none of these genes displayed obvious neoblast expression patterns, *erk-1*, *lkb1*, and *ampk* were noticeably decreased after 6,000 rad (Figures 4A, S5A, and S5B). Double FISH with *smedwi-1* confirmed that *erk-1*, *lkb1*, and *ampk* were expressed in neoblasts (Figures 4B and S5C). To determine whether any of these downstream effectors were required for neoblast repopulation, we subjected RNAi-treated animals to sublethal irradiation (1,250 rad). *erk-1(RNAi)* planarians displayed normal neoblast repopulation (Figures S5D–S5G). However, *lkb1(RNAi)* and *ampk(RNAi)* showed disrupted neoblast repopulation (Figures 4C–4F). Similar to *egfr-3(RNAi)*, unirradiated *lkb1(RNAi)* and *ampk(RNAi)* planarians maintained normal levels of neoblasts and proliferating cells (Figures 4G–4I). These

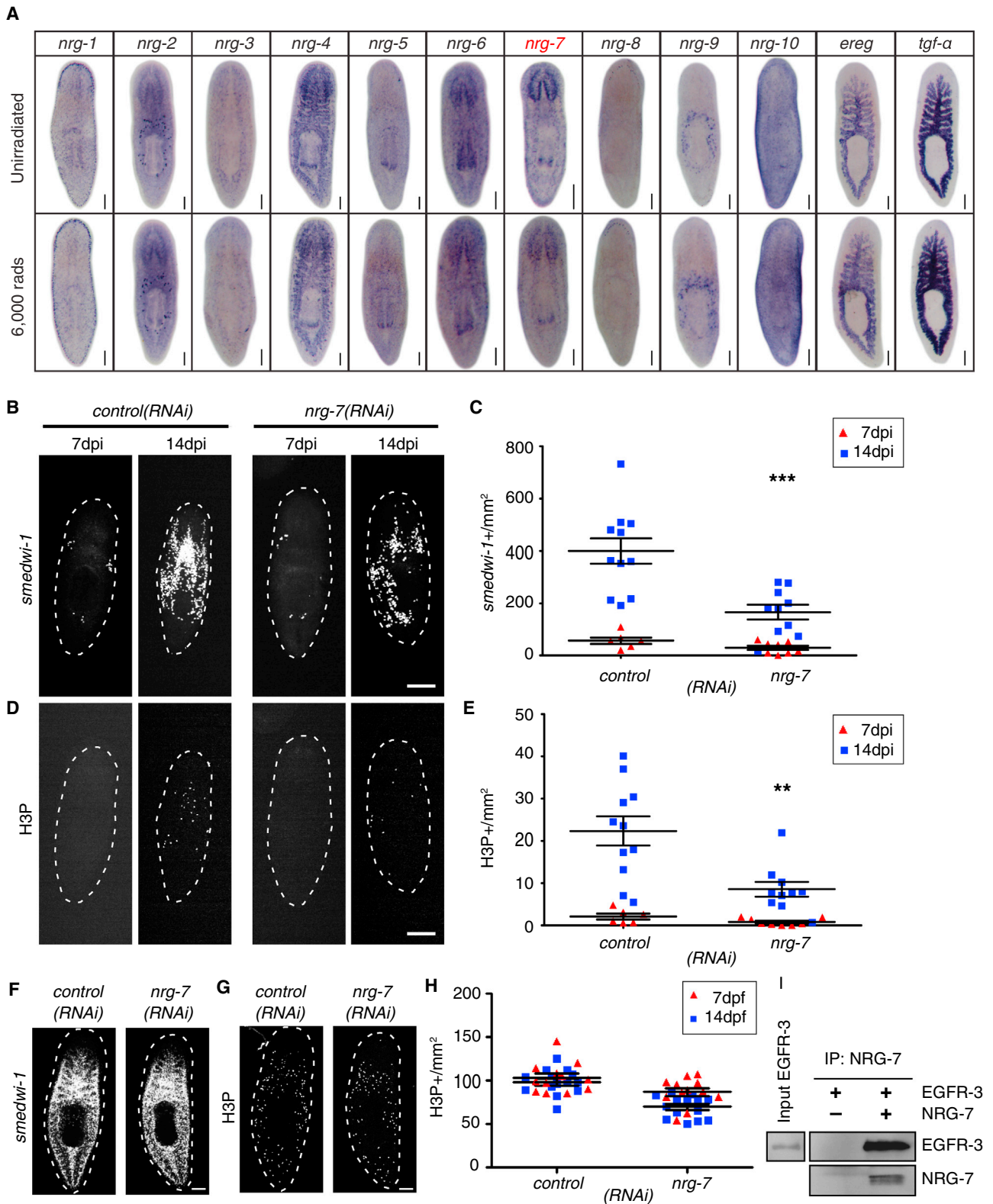


Figure 3. *nrg-7* Is Required for Neoblast Repopulation after Sublethal Irradiation

(A) WISH of putative *egf* ligands in unirradiated and 6,000-rad irradiated (1 dpi) planarians.

(B) FISH for *smedwi-1* in *control(RNAi)* and *nrg-7(RNAi)* planarians at 7 and 14 dpi.

(C) Quantification of *smedwi-1*⁺ cells/mm² in *nrg-7(RNAi)* animals. ****p* < 0.001.

(legend continued on next page)

carried out to compare the gene expression in neoblasts (Figure 5C). Candidate genes were cloned and WISH was performed to determine whether they were expressed in neoblasts. In the end, 27 genes were verified to be expressed in neoblasts (Figure 5D). Furthermore, FISH was performed to determine whether gene expression was affected in *egfr-3(RNAi)* compared with *control(RNAi)* animals. The data revealed that a DNA-damage repair gene *rad54b* (Hiramoto et al., 1999) was significantly downregulated in *egfr-3(RNAi)* compared with *control(RNAi)* animals (Figures 5E and 5F). Knockdown of *rad54b* impaired the dynamics of neoblast repopulation without affecting neoblast homeostasis (Figure 6). These results suggest that *egfr-3* regulates the expression of *rad54b* during neoblast repopulation and functionally associates aspects of DNA repair with EGF signaling. Because EGFR and lkb1-ampk have been found to be associated with DNA-damage repair in other systems (Chen and Nirodi, 2007; Sanli et al., 2014; Mahajan and Mahajan, 2015), the regulatory role of EGFR-3 in DNA damage is likely to be conserved in planarians in maintaining genome stability and ushering neoblast repopulation. Recently, another essential DNA-damage repair gene, *rad51*, was characterized in planarians to be required for DNA integrity, cell proliferation, and cell apoptosis during cell turnover (Peiris et al., 2016). Neoblasts could not recover in *rad51(RNAi)* animals after sublethal irradiation (Peiris et al., 2016), which is consistent with our study of *rad54b*, a *rad51* functional partner. This suggests that DNA-damage response and repair pathways are conserved in planarians, and future studies will explore the mechanism by which planarians maintain their genome stability through incessant cell proliferation.

Egfr-3 Regulates Asymmetric Cell Division in Neoblast Repopulation

To understand how *egfr-3* regulated neoblast repopulation after sublethal irradiation, we sought to determine the subcellular localization of EGFR-3 protein in neoblasts. cDNA of *egfr-3* was cloned from *Schmidtea mediterranea* and co-transfected along with EGFP-H1b, a nuclear marker, or Frizzled4-GFP, a cytoplasmic membrane marker, in 293T cells. Immunofluorescent staining showed clear cytoplasmic membrane localization of EGFR-3, consistent with its SMART structure prediction (Figures S7A–S7C). Next, an anti-EGFR-3 antibody was raised to determine the subcellular localization of EGFR-3 in vivo. Western blot of lysate from *egfr-3* transfected cells and *egfr-3(RNAi)* planarians verified the specificity of the antibody (Figures S7D–S7I). Together with *smedwi-1* in situ hybridization, it was clear that EGFR-3 was mainly expressed on the cytoplasmic membrane of neoblasts in *control(RNAi)* planarians (Figure 7A). As expected, EGFR-3 could not be detected in *egfr-3(RNAi)* neoblasts (Figure 7A). These results confirm that

Smed-egfr-3 codes for a cytoplasmic membrane protein in planarian neoblasts.

Further analysis of EGFR-3 subcellular localization uncovered an asymmetric distribution of this protein on the cytoplasmic membrane of neoblasts (Figure 7A). We hypothesized that *egfr-3* likely regulates neoblast repopulation by controlling asymmetric versus symmetric cell division. To test this idea, we first examined the distribution of EGFR-3 in dividing cells and found that EGFR-3 distribution was associated with symmetric/asymmetric distribution of *smedwi-1* transcripts (Figures 7B and 7C). We next examined anti-H3P⁺ dividing cells at mitotic anaphase and telophase during homeostasis and neoblast repopulation and analyzed the symmetric and asymmetric cell division based on the distribution of *smedwi-1* transcripts (Figures S7J–S7L). Both symmetric and asymmetric cell divisions were found in unirradiated and sublethally irradiated *control(RNAi)* animals (Figures 7D and S7M). To our surprise, asymmetric but not symmetric cell divisions were markedly decreased in sublethally irradiated *egfr-3(RNAi)* and *nrg-7(RNAi)* animals (Figure 7D, $p = 0.0055$ and $p = 0.0199$, respectively), suggesting that *egfr-3* promotes asymmetric cell division during neoblast repopulation. The direct consequence of symmetric and asymmetric cell division in neoblasts remains to be further characterized. However, a neoblast-specific organelle known as the chromatoid body also displays symmetric or asymmetric distribution in dividing cell pairs (Figure 8A), which is consistent with *smedwi-1* distribution. Asymmetric cell divisions shown with chromatoid bodies were also markedly decreased in sublethally irradiated *egfr-3(RNAi)* animals (Figure 8A, $p = 0.0449$), suggesting disturbed cell-fate regulation in *egfr-3(RNAi)* animals. A previous study reported that *egfr-3* functions in cell differentiation during head regeneration after amputation (Fraguas et al., 2011). Therefore, we suspected that *egfr-3* may also function in cell differentiation during neoblast repopulation. The density of *prog-1*⁺ cells was measured and the ratio of [*prog-1*⁺]/[*smedwi-1*⁺] at 14 dpi was significantly lower in *egfr-3(RNAi)* compared with controls, suggesting a defect in *prog-1*⁺ cell differentiation in *egfr-3(RNAi)* planarians (Figure S8). These results suggest that *egfr-3* might regulate neoblast repopulation and their subsequent differentiation by controlling asymmetric cell division.

We must emphasize that even though the ratio of asymmetric versus symmetric cell division changed, the total number of mitotic events during neoblast repopulation also decreases in *egfr-3(RNAi)* animals (see Figures 1H and 1I). Although we can only speculate as to why the cells fail to expand under a symmetric cell division strategy, the most likely explanation may be that the necessary post-mitotic progeny fail to form and signals likely supporting the neoblasts proper made by these cells are absent. We have seen similar outcomes already for two different RNAi treatments in the past: *smedwi-2* (Reddien et al., 2005) and

(D) Immunostaining with anti-H3P antibody in *control(RNAi)* and *nrg-7(RNAi)* planarians at 7 and 14 dpi.

(E) Quantification of H3P⁺ cells/mm² in *nrg-7(RNAi)* planarians. ** $p < 0.01$.

(F) FISH for *smedwi-1* in *control(RNAi)* and *nrg-7(RNAi)* unirradiated planarians at 14 days post feeding.

(G) Immunostaining with anti-H3P antibody in *control(RNAi)* and *nrg-7(RNAi)* unirradiated planarians.

(H) Quantification of H3P⁺ cells/mm² in *nrg-7(RNAi)* compared with *control(RNAi)*.

(I) Purified recombinant MYC-NRG-7-HIS (NRG-7) and the extracellular domain of FLAG-EGFR-3-HIS (EGFR-3) (residues 1–818) were incubated together and NRG-7 was captured using anti-MYC affinity resin. EGFR-3 and NRG-7 are detected only in the experimental reaction containing NRG-7.

Scale bars represent 200 μm (A, B, D) and 500 μm (F, G). See also Figure S4.

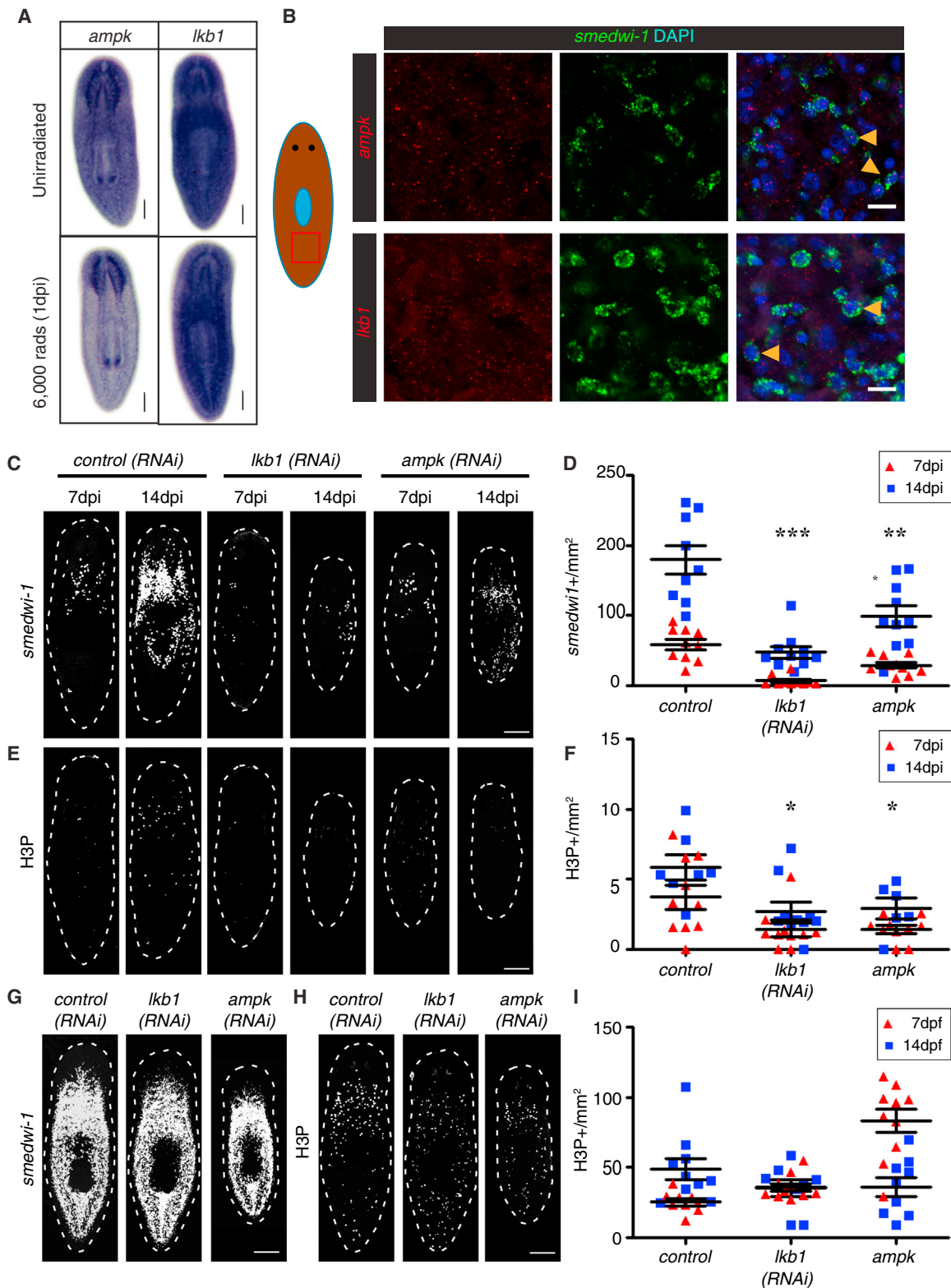


Figure 4. LKB1-AMPK Signaling Is Required for Neoblast Repopulation

(A) WISH for *ampk* and *lkb1* in unirradiated and 6,000-rad irradiated planarians.

(B) FISH for *ampk* and *lkb1* (red) in *smedwi-1*⁺ neoblasts (green). The orange arrowheads indicate *smedwi-1*⁺ neoblasts co-expressing *ampk* or *lkb1*.

(C) FISH for *smedwi-1* in *control*(RNAi), *ampk*(RNAi), and *lkb1*(RNAi) animals at 7 and 14 dpi.

(legend continued on next page)

p53 (Pearson et al., 2009). Under both of these conditions, the neoblasts are initially not affected in their capacity to proliferate but eventually, as the neoblasts fail to generate normal post-mitotic progeny, the neoblast population becomes exhausted and disappears. As such, it is likely that a hypothetical differentiation factor may be normally distributed to the opposite poles leading to asymmetric cell division, but that in *egfr3(RNAi)*-treated animals such asymmetry does not occur. This idea is supported by the fact that we observed the distribution of the cytoplasmic chromatoid bodies to be affected in *egfr-3(RNAi)* animals (Figure 8A). However, we cannot exclude the possibility that *egfr-3* regulates both cell cycle and asymmetric cell division independently through *lkb1/ampk* and *rad54b* or other unidentified factors. Taken together, our studies have led us to propose a model in which *egfr-3* regulates cell proliferation and asymmetric cell division during neoblast repopulation (Figures 8B and 8C).

DISCUSSION

Planarians Are a Powerful System to Study Signaling Regulation of Stem Cell Expansion In Vivo

How does the organism instruct stem cells to produce the correct types and numbers of cells to maintain normal tissue homeostasis? How do stem cells regulate the balance between self-renewal and the production of post-mitotic division progeny? How do stem cells control their expansion during regeneration? The relatively large abundance of a constantly cycling population of pluripotent stem cells in planarians (Newmark and Sánchez Alvarado, 2000; Wagner et al., 2011) provides a robust and experimentally accessible in vivo setting in which to examine fundamental problems of proliferative dynamics.

In humans, resident stem cells have been shown to facilitate homeostasis in many adult tissues (Biteau et al., 2011). However, their population dynamics and contributions to regeneration after tissue damage remain challenging to study (van Es et al., 2012; Vaughan et al., 2015; Zuo et al., 2015). Animal model systems help to overcome the difficulties by enabling the molecular and genetic dissection of stem cell biology. In particular, the abundance, experimental accessibility, and remarkable pluripotency of planarian neoblasts make this animal a tantalizing in vivo system for investigating fundamental questions of stem cell biology (Newmark and Sánchez Alvarado, 2000; Wagner et al., 2011). How, for instance, does the organism instruct stem cells to produce the correct types and numbers of cells during tissue homeostasis and regeneration? How do stem cells regulate the balance between self-renewal and the production of post-mitotic division progeny? How do planarians achieve all this without developing stem cell-associated diseases observed in other animals, such as cancer?

By using sublethal irradiation to induce clonal expansion of planarian neoblasts (Wagner et al., 2011), we tested the role of conserved signaling pathways in regulating this process. We identified a specific role for the EGF pathway in modulating the expansion of neoblasts, further demonstrating the utility of planarians for studying the behavior and functions of adult stem cells in vivo.

The EGF Signaling Pathway Regulates Planarian Stem Cell Expansion

In *S. mediterranea*, four EGFRs have been identified: *egfr-1*, *egfr-2*, *egfr-3*, and *egfr-5*. All these genes are expressed in differentiated tissues, but *egfr-3* distinguishes itself by also being expressed in neoblasts (Fraguas et al., 2011; Rink et al., 2011). Interestingly, loss of *egfr-3* expression affects cephalic regeneration and has been suggested to play a role in modulating neoblast functions (Fraguas et al., 2011). However, a direct role for *egfr-3* in regulating neoblast proliferation had not been demonstrated, and RNAi screens aimed at identifying modulators of stem cell proliferation did not include this gene, likely because its expression is not confined exclusively to neoblasts (Wagner et al., 2012). Because our study used a candidate approach to identify extracellular signals capable of modulating neoblast repopulation, *egfr-3* was included as a candidate in our RNAi screen. Given that under normal, homeostatic conditions RNAi of either *egfr-3* or its putative ligand *nrg-7* did not result in detectable defects, our findings suggest that EGFR-3/NGR-7 are not required for the maintenance of neoblasts, but may instead have a specialized role in the expansion and/or self-renewal of stem cells.

Multiple Cytokine Sources Regulate Tissue Homeostasis, Regeneration, and Neoblast Repopulation

In most studied species, stem cell activities are greatly influenced by diverse cytokines or niche signals (Forbes and Rosenthal, 2014). Our finding that loss of *egfr-3* and *nrg-7* via RNAi resulted in a repopulation-specific neoblast deficiency indicates that a high degree of specialization of signaling molecules and their pathways must exist in planarians. Planarian muscle cells have recently been shown to serve as signaling centers capable of generating multiple factors for tissue regeneration and turnover (Witchley et al., 2013), and neuropeptides (Baguña et al., 1989a, 1989b; Saló and Baguña, 1986) and Hedgehog expressed in the nervous system (Rink et al., 2009; Yazawa et al., 2009) have been shown to affect neoblast division rates. Cells undergoing differentiation have also been reported to affect the maintenance and dynamics of the neoblast population (Tu et al., 2015; Zhu et al., 2015). Our finding that *nrg-7* is expressed in *prog-1⁺* cells and *PC2⁺* neuron cells (Figure S4K) provides additional cytokine sources regulating neoblasts in planarians.

(D) Quantification of *smcdwi-1⁺* cells/mm² in *ampk(RNAi)* and *lkb1(RNAi)* planarians. **p < 0.01, ***p < 0.001.

(E) Immunostaining with anti-H3P antibody in *control(RNAi)*, *ampk(RNAi)*, and *lkb1(RNAi)* planarians at 7 and 14 dpi.

(F) Quantification of H3P⁺ cells/mm² in *ampk(RNAi)* and *lkb1(RNAi)* planarians. *p < 0.05.

(G) FISH for *smcdwi-1* in *control(RNAi)*, *ampk(RNAi)*, and *lkb1(RNAi)* unirradiated animals.

(H) Immunostaining with anti-H3P antibody in *control(RNAi)*, *ampk(RNAi)*, and *lkb1(RNAi)* unirradiated animals.

(I) Quantification of H3P⁺ cells/mm² shows no significant reduction in proliferating cells in *ampk(RNAi)* and *lkb1(RNAi)* compared with controls.

Scale bars, 200 μm (A, C, E, G, H), 20 μm (B). See also Figure S5.

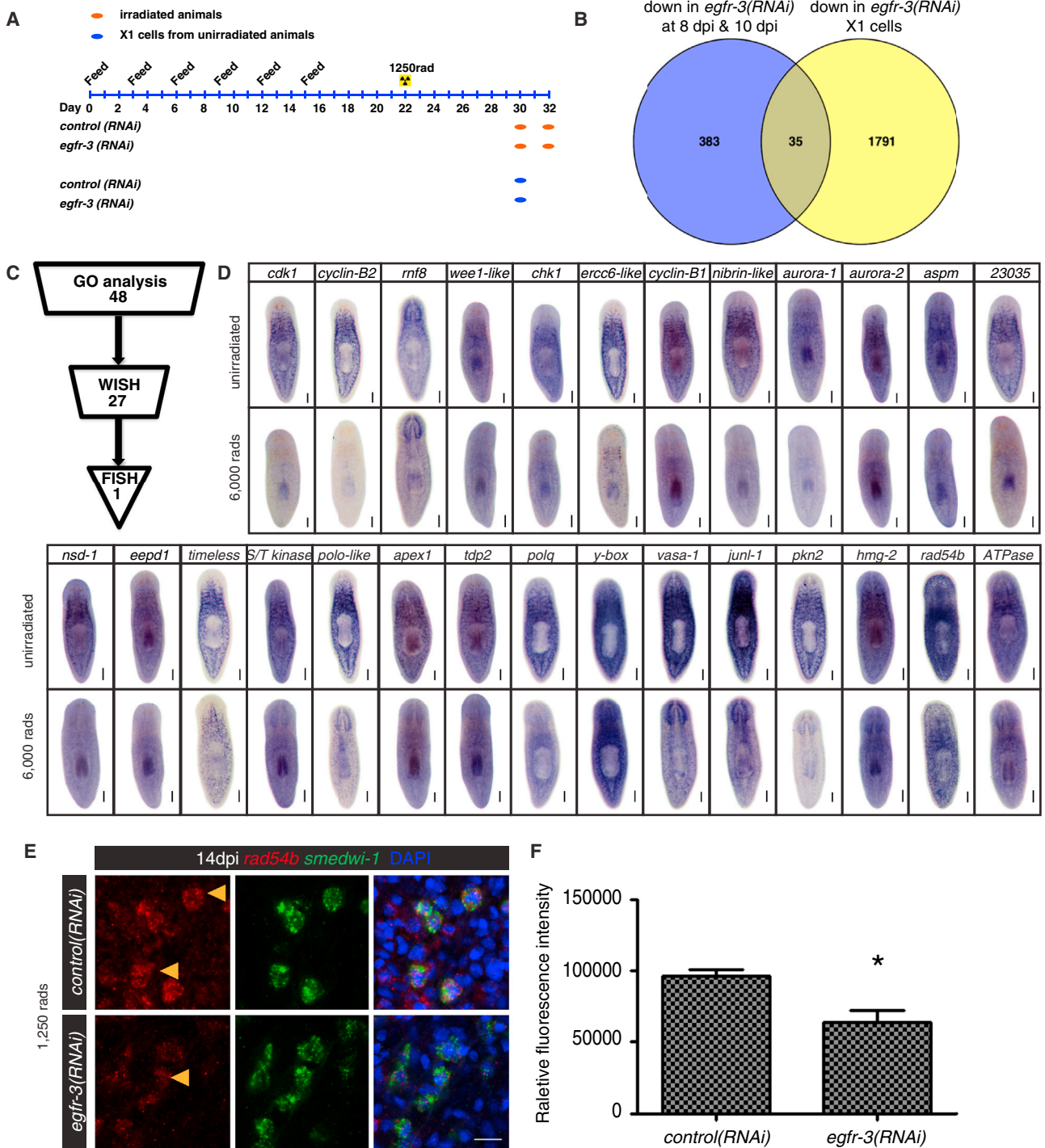


Figure 5. RNA-Seq Analysis of *egfr-3(RNAi)* in Neoblast Repopulation

(A) Feeding schedule and sample collection of *control(RNAi)* and *egfr-3(RNAi)* planarians for RNA-seq.
 (B) Venn diagram showing differentially expressed genes in *egfr-3(RNAi)* compared with *control(RNAi)* planarians at 8 and 10 dpi, and in X1 cells of unirradiated animals.
 (C) Procedure for identifying the *egfr-3* regulated gene including gene ontology analysis, WISH, and FISH.
 (D) WISH of candidate genes in unirradiated and 6,000-rad irradiated planarians. Scale bars, 200 μ m.
 (E) FISH for *rad54b* (red) in *smedwi-1⁺* neoblasts (green). The orange arrowheads indicate cells expressing *rad54b*. Scale bar, 20 μ m.
 (F) Histogram showing *rad54b* fluorescence intensity in *control(RNAi)* and *egfr-3(RNAi)* planarians. * $p < 0.05$.
 See also [Figure S6](#); [Tables S1](#) and [S2](#).

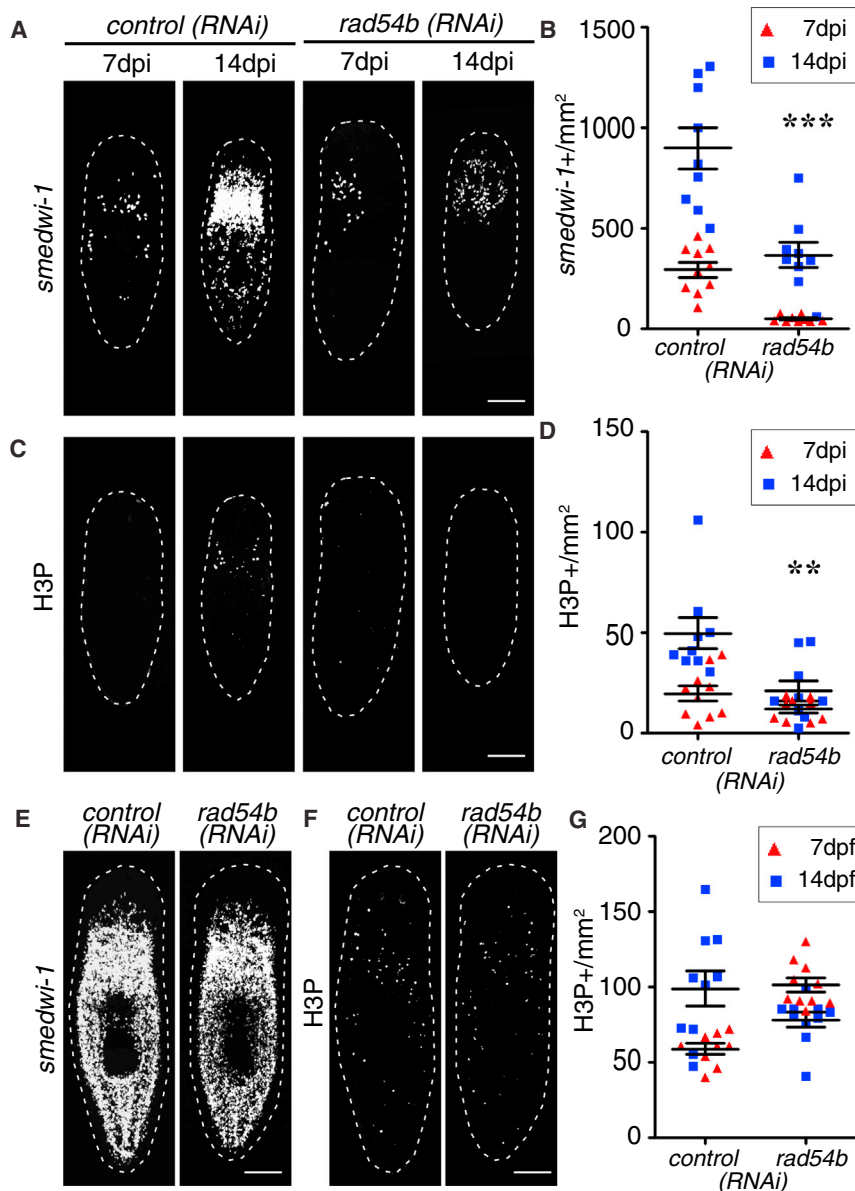


Figure 6. *rad54b* Is Required for Neoblast Repopulation

(A) FISH for *smedwi-1* in *control(RNAi)* and *rad54b(RNAi)* planarians at 7 and 14 dpi. (B) Quantification of *smedwi-1*⁺ cells/mm² in *rad54b(RNAi)* planarians. ****p* < 0.001. (C) Immunostaining with anti-H3P antibody in *control(RNAi)* and *rad54b(RNAi)* planarians at 7 and 14 dpi. (D) Quantification of H3P⁺ cells/mm² in *rad54b(RNAi)* planarians. ***p* < 0.01. (E) FISH for *smedwi-1* in *control(RNAi)* and *rad54b(RNAi)* unirradiated animals. (F) Immunostaining with anti-H3P antibody in *control(RNAi)* and *rad54b(RNAi)* unirradiated animals. (G) Quantification of H3P⁺ cells/mm² shows no significant reduction in proliferating cells in *rad54b(RNAi)* compared with controls. Scale bars, 200 μm (A, C, E, F).

Interestingly, the complex molecular heterogeneity of planarian stem cells can be restored by the proliferation of the very few neoblasts surviving after sublethal irradiation, and with some frequency by single transplanted neoblasts (Wagner et al., 2011, 2012). These two experimental approaches have led to postulation for the existence of a clonogenic or cNeoblast (Wagner et al., 2011). Furthermore, during the colony expansion following sublethal irradiation, a spliced leader RNA SL3 was found to be expressed in all neoblasts of small colonies (<6 neoblasts), but only expressed in subsets of neoblasts of bigger colonies (>8 neoblasts) (Rossi et al., 2013), supporting the idea that developmental mechanisms likely drive the molecular heterogeneity of the neoblast population (Reddien, 2013). It is not clear, however, whether asymmetric cell division functions in the generation of specialized neoblasts from cNeoblasts.

EGFR-3 Signaling Is Required for Asymmetric versus Symmetric Cell Division in Neoblasts during Neoblast Repopulation

Adult stem cells rely on asymmetric cell division for both self-renewal and generation of differentiated progeny, a process that allows organisms to precisely maintain stem cell numbers and regulate somatic cell turnover (Inaba and Yamashita, 2012). While asymmetric cell division has long been proposed to exist in planarians (Reddien, 2013; Rink, 2013), there has been no direct evidence supporting its existence until now. As in tissue homeostasis, precise regulation of stem cell self-renewal and differentiation is also required for regeneration (Tanaka and Reddien, 2011). Hence, molecular heterogeneity of the stem cell population in planarians is to be expected, and has begun to be uncovered in recent studies (Hayashi et al., 2006; Lapan and Reddien, 2011; Pearson and Sánchez Alvarado, 2010; Tu et al., 2015; van Wolfswinkel et al., 2014).

Here we show that *smedwi-1* mRNA and chromatoid bodies display both symmetric and asymmetric distribution in dividing neoblasts during homeostasis (Figures 7D, S7M, and 8A). *egfr-3(RNAi)* did not noticeably alter the ~1:1 ratio of symmetric to asymmetric cell divisions in unirradiated animals (Figure S7M). However, after sublethal irradiation asymmetric cell divisions were impaired in *egfr-3(RNAi)* animals (Figure 7D), drastically affecting neoblast repopulation and the production of a specialized lineage (Figures 1F–1I and S8). This is the first functional demonstration of a role for asymmetric cell division in stem cell function in planarians. Altogether, we propose a model in which the observed asymmetric distribution of EGFR-3 (Figures 7A and 7B) is required for the proliferation and differentiation of neoblasts surviving from sublethal irradiation into lineage-specified neoblasts (Figure 8C). In the future, experiments aimed at determining the requirement of asymmetric cell division in the

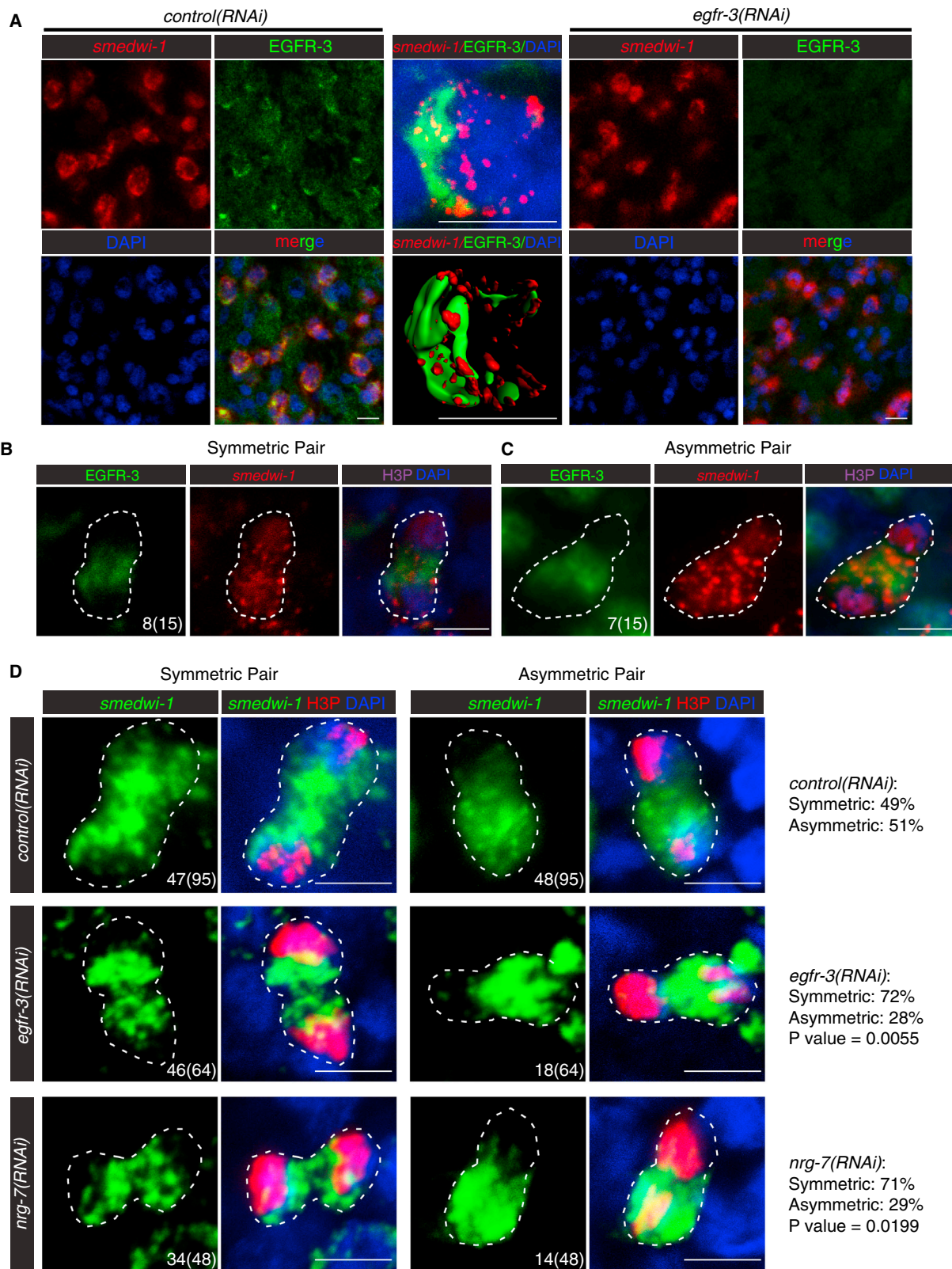


Figure 7. Knockdown of *egfr-3* Reduces Asymmetric Cell Division during Neoblast Repopulation after Sublethal Irradiation

(A) Immunostaining with an antibody against EGFR-3 in *control(RNAi)* planarians. *Egfr-3* knockdown eliminates the staining. (B) Representative images showing EGFR-3 and *smedwi-1* distribution in symmetric cell division.

(legend continued on next page)

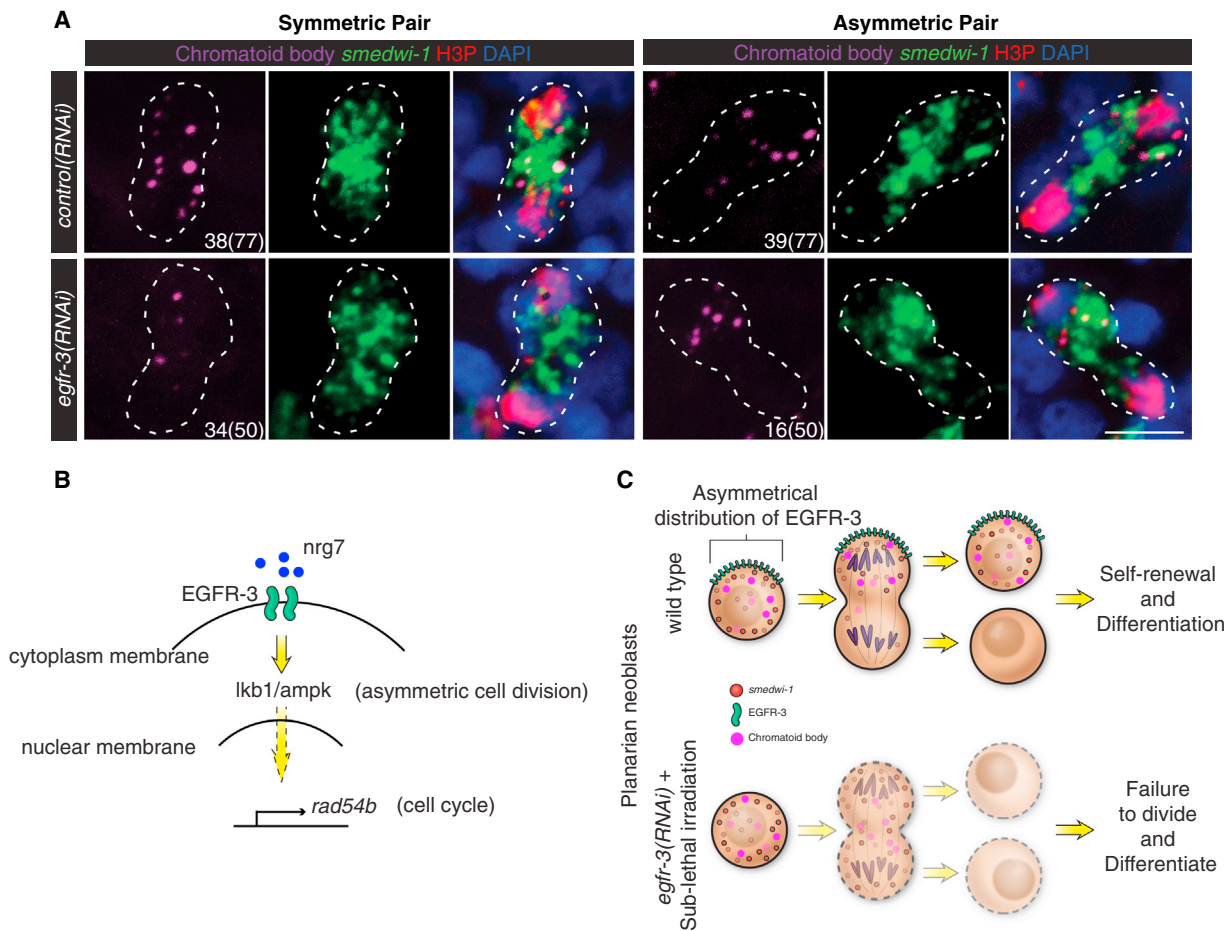


Figure 8. Asymmetric Distribution of Chromatoid Body in Dividing Cells Is Impaired in *egfr-3*(RNAi) Animals during Neoblast Repopulation after Sublethal Irradiation

(A) Representative images and numbers of asymmetric versus symmetric cell divisions observed in *control*(RNAi) and *egfr-3*(RNAi) planarians at 14 dpi based upon distribution of chromatoid bodies (anti-Y-12* antibody, purple), and *smedwi-1* RNA (green). $p = 0.0449$. Dividing cells are labeled with anti-H3P antibody (red), and nuclei are stained with DAPI (blue). Scale bar, 10 μ m.

(B) EGF signaling regulation of asymmetric cell division and cell cycle through *nrg-7*, *egfr-3*, *lkb1/ampk*, and *rad54b* during neoblast repopulation after sublethal irradiation.

(C) Proposed model of EGF signaling in asymmetric cell division in planaria.

See also Figure S8.

ontogeny of the observed neoblast heterogeneity in planarians will help shed light on how this remarkable population of adult stem cells regulates its dynamics.

The Role of EGF Signaling in Regulating Asymmetric Stem Cell Division and Repopulation Is Likely Evolutionarily Ancient

Asymmetric distribution of EGFR in stem cells was first described in mice, in which adult neural stem cells are regulated by the asymmetric distribution of EGFR (Sun et al., 2005). In the mouse brain, *Egfr* is required for both maintaining adult stem cells in the subventricular zone (Suh et al., 2009) and generating

CNS progenitor cells (Sun et al., 2005). *egfr* is also required in *Drosophila* for intestinal stem cell proliferation and midgut regeneration (Jiang et al., 2011), maintenance of the germline niche architecture (Chen et al., 2013), and self-renewal and establishment of the cell polarity of epidermal follicle stem cells (Castanieto et al., 2014). The discovery in the Lophotrochozoa (e.g., planarians), a sister group to the Deuterostomes (e.g., vertebrates) and the Ecdysozoa (e.g., *Drosophila*), of the asymmetric distribution of EGFR-3 in stem cells (Figure 7A) and the role it plays in the asymmetric production of daughter cells (Figures 7B–7D), indicates an ancient evolutionary origin for these functions.

(C) Representative images showing EGFR-3 and *smedwi-1* distribution in asymmetric cell division.

(D) Representative images and numbers of asymmetric versus symmetric cell divisions in *control*(RNAi), *egfr-3*(RNAi), and *nrg-7*(RNAi) planarians at 14 dpi.

Scale bars, 10 μ m. p Value calculated for *egfr-3*(RNAi) versus *control*(RNAi) and *nrg-7*(RNAi) versus *control*(RNAi), respectively, using two-tailed Fisher's exact test. See also Figure S7.

Such conservation may be intricately associated with the evolution of cell polarity in complex tissues. A recent study in *Drosophila* revealed that asymmetric EGFR distribution in follicle stem cells is required for the establishment of cell polarity via ERK and liver kinase B1 (LKB1)-AMP-activated protein kinase (AMPK) and for the proper localization of the Par-PKC-Baz cell polarity complex, which disappeared when *egfr* was mutated (Castanieto et al., 2014). Our study also suggests a similar role for LKB1-AMPK. RNAi of these genes in sublethally irradiated animals affected neoblast repopulation in a manner indistinguishable from that in *egfr-3(RNAi)*-treated animals. However, it remains to be determined whether EGFR-3 regulates LKB1-AMPK directly or indirectly. Moreover, *lkb1* and *ampk* function in planarians may be pleiotropic, as suggested by the broad expression of these genes and the reduction in animal size observed in unirradiated animals during homeostasis (Figure 4). Exploring the possible roles of planarian *egfr-3* in the conserved hierarchy of polarity establishment and maintenance, along with the identification and characterization of additional mitogen-activated protein kinases, will be the focus of future investigations.

Egfr-3 May Be a Regulator of Genomic Stability during Neoblast Expansion

The mechanisms by which the lifelong maintenance of the neoblast population in planarians is regulated and how these cells are kept from uncontrolled hyperproliferation and genomic instability remain unknown. Our analyses of the genomic output modulated by *egfr-3* identified not only expected regulators of the cell cycle (e.g., *cyclin b*, *cyclin dependent kinase 1*), but also DNA-damage response genes (*rad54b*, *rnf8*, *p53*, *DNA lyase*). The link between *egfr-3*, DNA-damage repair, and asymmetric cell divisions suggests the intriguing possibility that a detection/checkpoint mechanism for asymmetric cell division may normally occur during neoblast proliferation, which may have been exacerbated by the DNA damage introduced by sublethal irradiation. Therefore, we hypothesize that the DNA-damage response and repair complex in neoblasts may be under EGF signaling regulation and may play an essential role in symmetric versus asymmetric cell divisions by maintaining planarian stem cell genomic stability, and mitigating normal cellular aging processes. Given our increasing ability to visualize DNA damage in planarian chromosomes (Xiang et al., 2014), future studies will aim to measure this process during neoblast proliferation and clonal expansion.

EXPERIMENTAL PROCEDURES

Planarian Culture and Irradiation Treatment

Asexual *S. mediterranea* (strain CIW4) were maintained at 20°C as previously described (Newmark and Sánchez Alvarado, 2000). For all experiments, animals were starved for 7–14 days. A GammaCell 40 Exactor irradiator exposed animals to either 1,250 or 6,000 rad for sublethal and lethal irradiations, respectively.

Molecular Cloning and RNAi Feeding

cDNAs of all tested genes were cloned into a pPR-T4P vector as described previously (Gurley et al., 2008). RNAi food was prepared by adding 125 μ L of liver paste (9 parts of liver to 1 part of water) into a bacterial pellet obtained from 50-mL overnight cultures. *Unc22*, a *Caenorhabditis elegans* gene without nucleotide sequence homology in planarians, was used as control RNAi.

Animals in all RNAi experiments were fed six times with 3 days between feedings. 1,250 rad of irradiation or amputation was carried out 7 or 4 days after the last feeding, respectively. Day 0 represents time of irradiation or amputation.

In Situ Hybridizations and Antibody Staining

In situ hybridizations were performed as previously described (King and Newmark, 2013; Pearson et al., 2009) with some modifications. Animals were fixed for 45 min in 4% formaldehyde, 0.5% Triton X-100, and 1 \times PBS. To improve optical clarity after signal development, we used Sca/A2 (Hama et al., 2011) with 80% glycerol and 4 M urea for colorimetric WISH. Glycerol (20%), DABCO (2.5%) (Sigma-Aldrich), and 4 M urea Sca/A2 with was used for FISH. Anti-phospho-histone H3 (Ser10) (H3P) antibody (1:1,000; Abcam, ab32107) and Alexa-conjugated goat anti-rabbit secondary antibodies (1:1,000; Abcam, ab150086) were used to stain proliferating cells at the G₂/M phase of the cell cycle.

Bromodeoxyuridine Labeling

Animals were soaked in 25 mg/mL BrdU (Fluka, Sigma-Aldrich) for 4 hr (van Wolfswinkel et al., 2014) and fixed at specified time points. In situ hybridization and BrdU antibody staining were performed as previously described (Thi-Kim Vu et al., 2015). BrdU was detected via a rat anti-BrdU antibody (1:1,000; Abcam, ab6326).

TUNEL Assay

Animals were fixed and stained with a TUNEL assay kit (Roche) as previously described (Pellettieri et al., 2010). TUNEL-stained specimens were imaged for quantification on a PerkinElmer Ultraview spinning-disc microscope.

Antibody Generation

The anti-EGFR-3 antibody was generated by YenZym Antibodies. We used a peptide antigen derived from EGFR-3 amino acids 361–376 to immunize rabbits. Polyclonal antibodies were affinity purified with a Hitrap NHS-activated HP column (GE Healthcare Life Sciences).

Microscopy

Colorimetric WISH images were captured using a Zeiss SteREO Lumar stereoscope. Confocal images were captured using either a Zeiss LSM-700 or a Zeiss LSM-510. For quantification, tiled images of individual worms were acquired using a PerkinElmer Ultraview spinning-disc microscope, then stitched and spots counted as described previously (Adler et al., 2014).

Protein In Vitro Binding Assay

Recombinant MYC-NRG-7-HIS was expressed in bacteria, and recombinant FLAG-EGFR-3-HIS extracellular domain (residues 1–818) was expressed in baculovirus. Proteins were affinity purified using standard methods with nickel affinity resin. To determine direct ligand/receptor interaction, we incubated NRG-7 and EGFR-3 along with Anti-c-Myc Agarose Affinity Gel (Sigma-Aldrich) with 100 ng/ μ L BSA in NETN buffer (250 mM NaCl, 5 mM EDTA, 50 mM Tris-HCl [pH 8.0], 0.5% NP-40, 10% glycerol, 1 mM DTT). After 1 hr at 4°C, the affinity resin was washed five times with 15 volumes of NETN. Bound proteins were eluted with 2 \times urea-based Laemmli buffer (50 mM Tris-HCl [pH 6.8], 1.6% SDS, 7% glycerol, 8 M urea, 4% β -mercaptoethanol, 0.016% bromophenol blue). Samples were heated for 10 min at 80°C and fractionated by SDS-PAGE for analysis.

Next-Generation RNA-Seq

Worms and sorted X1 cells were homogenized in TRIzol (Life Technologies), and RNA isolated according to the manufacturer's protocol. Approximately 100 ng of RNA per sample were used for library generation using the Illumina TruSeq kit. Libraries were sequenced in 50-bp single reads using an Illumina HiSeq 2500 sequencer. A set of 43,806 predicted *S. mediterranea* transcripts were used to analyze the RNA-seq data (Robb et al., 2015).

Statistical Analyses

A two-tailed Fisher's exact test was performed for statistical analyses of symmetric versus asymmetric cell divisions. All other statistical analyses were performed using Student's t test. $p < 0.05$ was considered a significant difference.

ACCESSION NUMBERS

The accession number for the RNA-seq data reported in this paper is GEO: GSE84025.

SUPPLEMENTAL INFORMATION

Supplemental Information includes eight figures and three tables and can be found with this article online at <http://dx.doi.org/10.1016/j.devcel.2016.07.012>.

AUTHOR CONTRIBUTIONS

Conceptualization, K.L. and A.S.A.; Methodology, K.L. and A.S.A.; Investigation, K.L., H.T.V., and R.D.M.; Formal Analysis, K.L., H.T.V., R.D.M., S.A.M., C.W.S., R.A., and K.G.; Writing – Original Draft, K.L. and A.S.A.; Writing – Review & Editing, K.L. and A.S.A.; Funding Acquisition, A.S.A.; Supervision, J.L.W. and A.S.A.

ACKNOWLEDGMENTS

We thank all members of the Sánchez Alvarado laboratory, especially Eric Ross, for bioinformatics assistance, Li-Chun Cheng, Carlos Guerrero Hernandez, and Aurimas Gumbrys for technical help and probes, and Sarah Elliott, Erin Davies, Kim Tu, Elizabeth Duncan, Christopher Arnold, and Stephanie Nowotarski for comments on the manuscript. We also thank Mark Miller for the illustration in Figure 8C, as well as Xin Qian and all members of the Reptile & Aquatics, Molecular Biology, Cytometry, Microscopy, and Histology Core Facilities at the Stowers Institute for Medical Research for technical support. This work was supported by NIH R37GM057260 to A.S.A., who is a Howard Hughes Medical Institute and a Stowers Institute for Medical Research investigator.

Received: December 14, 2015

Revised: June 1, 2016

Accepted: July 15, 2016

Published: August 11, 2016

REFERENCES

Adell, T., Saló, E., Boutros, M., and Bartscherer, K. (2009). Smed-Evi/Wntless is required for β -catenin-dependent and -independent processes during planarian regeneration. *Development* 136, 905–910.

Adler, C.E., Seidel, C.W., McKinney, S.A., and Sánchez Alvarado, A. (2014). Selective amputation of the pharynx identifies a FoxA-dependent regeneration program in planaria. *Elife* 3, e02238.

Alberts, B., Johnson, A., Lewis, J., Raff, M., Roberts, K., and Walter, P. (2002). Extracellular control of cell division, cell growth, and apoptosis. In *Molecular Biology of the Cell*, Fourth Edition (New York: Garland Science).

Baguña, J., Saló, E., and Auladell, C. (1989a). Regeneration and pattern formation in planarians. III. Evidence that neoblasts are totipotent stem cells and the source of blastema cells. *Development* 107, 77–86.

Baguña, J., Saló, E., and Romero, R. (1989b). Effects of activators and antagonists of the neuropeptides substance P and substance K on cell proliferation in planarians. *Int. J. Dev. Biol.* 33, 261–266.

Bardeen, C., and Baetjer, F. (1904). The inhibitive action of the Roentgen rays on regeneration in planarians. *J. Exp. Zool.* 1, 5.

Biteau, B., Hochmuth, C.E., and Jasper, H. (2011). Maintaining tissue homeostasis: dynamic control of somatic stem cell activity. *Cell Stem Cell* 9, 402–411.

Castanieto, A., Johnston, M.J., and Nystul, T.G. (2014). EGFR signaling promotes self-renewal through the establishment of cell polarity in *Drosophila* follicle stem cells. *Elife* 3, e04437.

Cebrià, F., Kobayashi, C., Umeson, Y., Nakazawa, M., Mineta, K., Ikeo, K., Gojobori, T., Itoh, M., Taira, M., Sánchez Alvarado, A., et al. (2002). FGFR-related gene *nou-darake* restricts brain tissues to the head region of planarians. *Nature* 419, 620–624.

Chen, D.J., and Nirodi, C.S. (2007). The epidermal growth factor receptor: a role in repair of radiation-induced DNA damage. *Clin. Cancer Res.* 13, 6555–6560.

Chen, H., Chen, X., and Zheng, Y. (2013). The nuclear lamina regulates germline stem cell niche organization via modulation of EGFR signaling. *Cell Stem Cell* 13, 73–86.

Coward, S.J. (1974). Chromatoid bodies in somatic cells of the planarian: observations on their behavior during mitosis. *Anat. Rec.* 180, 533–545.

Forbes, S.J., and Rosenthal, N. (2014). Preparing the ground for tissue regeneration: from mechanism to therapy. *Nat. Med.* 20, 857–869.

Fraguas, S., Barberan, S., and Cebrià, F. (2011). EGFR signaling regulates cell proliferation, differentiation and morphogenesis during planarian regeneration and homeostasis. *Dev. Biol.* 354, 87–101.

Gaviño, M.A., and Reddien, P.W. (2011). A Bmp/Admp regulatory circuit controls maintenance and regeneration of dorsal-ventral polarity in planarians. *Curr. Biol.* 21, 294–299.

Gaviño, M.A., Wenemoser, D., Wang, I.E., and Reddien, P.W. (2013). Tissue absence initiates regeneration through Follistatin-mediated inhibition of Activin signaling. *Elife* 2, e00247.

Guedelhoefer, O.C., and Sánchez Alvarado, A. (2012). Amputation induces stem cell mobilization to sites of injury during planarian regeneration. *Development* 139, 3510–3520.

Gurley, K.A., Rink, J.C., and Sánchez Alvarado, A. (2008). Beta-catenin defines head versus tail identity during planarian regeneration and homeostasis. *Science* 319, 323–327.

Hama, H., Kurokawa, H., Kawano, H., Ando, R., Shimogori, T., Noda, H., Fukami, K., Sakaue-Sawano, A., and Miyawaki, A. (2011). Scale: a chemical approach for fluorescence imaging and reconstruction of transparent mouse brain. *Nat. Neurosci.* 14, 1481–1488.

Hayashi, T., Asami, M., Higuchi, S., Shibata, N., and Agata, K. (2006). Isolation of planarian X-ray-sensitive stem cells by fluorescence-activated cell sorting. *Dev. Growth Differ.* 48, 371–380.

Hiramoto, T., Nakanishi, T., Sumiyoshi, T., Fukuda, T., Matsuura, S., Tauchi, H., Komatsu, K., Shibasaki, Y., Inui, H., Watatani, M., et al. (1999). Mutations of a novel human RAD54 homologue, RAD54B, in primary cancer. *Oncogene* 18, 3422–3426.

Hogan, B.L., Barkauskas, C.E., Chapman, H.A., Epstein, J.A., Jain, R., Hsia, C.C., Niklason, L., Calle, E., Le, A., Randell, S.H., et al. (2014). Repair and regeneration of the respiratory system: complexity, plasticity, and mechanisms of lung stem cell function. *Cell Stem Cell* 15, 123–138.

Hsu, Y.C., and Fuchs, E. (2012). A family business: stem cell progeny join the niche to regulate homeostasis. *Nat. Rev. Mol. Cell Biol.* 13, 103–114.

Iglesias, M., Gomez-Skarmeta, J.L., Saló, E., and Adell, T. (2008). Silencing of Smed-betacatenin1 generates radial-like hypercephalized planarians. *Development* 135, 1215–1221.

Inaba, M., and Yamashita, Y.M. (2012). Asymmetric stem cell division: precision for robustness. *Cell Stem Cell* 11, 461–469.

Jiang, H., Grenley, M.O., Bravo, M.J., Blumhagen, R.Z., and Edgar, B.A. (2011). EGFR/Ras/MAPK signaling mediates adult midgut epithelial homeostasis and regeneration in *Drosophila*. *Cell Stem Cell* 8, 84–95.

King, R.S., and Newmark, P.A. (2013). In situ hybridization protocol for enhanced detection of gene expression in the planarian *Schmidtea mediterranea*. *BMC Dev. Biol.* 13, 8.

Kobayashi, C., Saito, Y., Ogawa, K., and Agata, K. (2007). Wnt signaling is required for antero-posterior patterning of the planarian brain. *Dev. Biol.* 306, 714–724.

Kotton, D.N., and Morrisey, E.E. (2014). Lung regeneration: mechanisms, applications and emerging stem cell populations. *Nat. Med.* 20, 822–832.

Lapan, S.W., and Reddien, P.W. (2011). Dlx and sp6-9 Control optic cup regeneration in a prototypic eye. *PLoS Genet.* 7, e1002226.

Mahajan, K., and Mahajan, N.P. (2015). Cross talk of tyrosine kinases with the DNA damage signaling pathways. *Nucleic Acids Res.* 43, 10588–10601.

- Mendelson, A., and Frenette, P.S. (2014). Hematopoietic stem cell niche maintenance during homeostasis and regeneration. *Nat. Med.* **20**, 833–846.
- Miller, C.M., and Newmark, P.A. (2012). An insulin-like peptide regulates size and adult stem cells in planarians. *Int. J. Dev. Biol.* **56**, 75–82.
- Miyajima, A., Tanaka, M., and Itoh, T. (2014). Stem/progenitor cells in liver development, homeostasis, regeneration, and reprogramming. *Cell Stem Cell* **14**, 561–574.
- Molina, M.D., Saló, E., and Cebrià, F. (2007). The BMP pathway is essential for re-specification and maintenance of the dorsoventral axis in regenerating and intact planarians. *Dev. Biol.* **311**, 79–94.
- Morgan, T. (1900). Regeneration in planarians. *Archiv. Entwickl. Mech.* **10**, 58–119.
- Morrison, S.J., and Kimble, J. (2006). Asymmetric and symmetric stem-cell divisions in development and cancer. *Nature* **441**, 1068–1074.
- Neumuller, R.A., and Knoblich, J.A. (2009). Dividing cellular asymmetry: asymmetric cell division and its implications for stem cells and cancer. *Genes Dev.* **23**, 2675–2699.
- Newmark, P.A., Reddien, P.W., Cebrià, F., and Sánchez Alvarado, A. (2003). Ingestion of bacterially expressed double-stranded RNA inhibits gene expression in planarians. *Proc. Natl. Acad. Sci. USA* **100** (Suppl 1), 11861–11865.
- Newmark, P.A., and Sánchez Alvarado, A. (2000). Bromodeoxyuridine specifically labels the regenerative stem cells of planarians. *Dev. Biol.* **220**, 142–153.
- Ogawa, K., Kobayashi, C., Hayashi, T., Orii, H., Watanabe, K., and Agata, K. (2002). Planarian fibroblast growth factor receptor homologs expressed in stem cells and cephalic ganglions. *Dev. Growth Differ.* **44**, 191–204.
- Pearson, B.J., and Sánchez Alvarado, A. (2010). A planarian p53 homolog regulates proliferation and self-renewal in adult stem cell lineages. *Development* **137**, 213–221.
- Pearson, B.J., Eisenhoffer, G.T., Gurley, K.A., Rink, J.C., Miller, D.E., and Sánchez Alvarado, A. (2009). Formaldehyde-based whole-mount in situ hybridization method for planarians. *Dev. Dyn.* **238**, 443–450.
- Pellettieri, J., Fitzgerald, P., Watanabe, S., Mancuso, J., Green, D.R., and Sánchez Alvarado, A. (2010). Cell death and tissue remodeling in planarian regeneration. *Dev. Biol.* **338**, 76–85.
- Peiris, T.H., Ramirez, D., Barghouth, P.G., Ofoha, U., Davidian, D., Weckerle, F., and Oviedo, N.J. (2016). Regional signals in the planarian body guide stem cell fate in the presence of DNA instability. *Development* **143**, 1697–1709.
- Petersen, C.P., and Reddien, P.W. (2008). Smed- β catenin-1 is required for anteroposterior blastema polarity in planarian regeneration. *Science* **319**, 327–330.
- Petersen, C.P., and Reddien, P.W. (2009). A wound-induced Wnt expression program controls planarian regeneration polarity. *Proc. Natl. Acad. Sci. USA* **106**, 17061–17066.
- Reddien, P.W. (2013). Specialized progenitors and regeneration. *Development* **140**, 951–957.
- Reddien, P.W., and Sánchez Alvarado, A. (2004). Fundamentals of planarian regeneration. *Annu. Rev. Cell Dev. Biol.* **20**, 725–757.
- Reddien, P.W., Oviedo, N.J., Jennings, J.R., Jenkin, J.C., and Sánchez Alvarado, A. (2005). SMEDWI-2 is a PIWI-like protein that regulates planarian stem cells. *Science* **310**, 1327–1330.
- Reddien, P.W., Bermange, A.L., Kicza, A.M., and Sánchez Alvarado, A. (2007). BMP signaling regulates the dorsal planarian midline and is needed for asymmetric regeneration. *Development* **134**, 4043–4051.
- Rink, J.C. (2013). Stem cell systems and regeneration in planaria. *Dev. Genes Evol.* **223**, 67–84.
- Rink, J.C., Gurley, K.A., Elliott, S.A., and Sánchez Alvarado, A. (2009). Planarian Hh signaling regulates regeneration polarity and links Hh pathway evolution to cilia. *Science* **326**, 1406–1410.
- Rink, J.C., Vu, H.T., and Sánchez Alvarado, A. (2011). The maintenance and regeneration of the planarian excretory system are regulated by EGFR signaling. *Development* **138**, 3769–3780.
- Robb, S.M., Gotting, K., Ross, E., and Sánchez Alvarado, A. (2015). SmedGD 2.0: the *Schmidtea mediterranea* genome database. *Genesis* **53**, 535–546.
- Roberts-Galbraith, R.H., and Newmark, P.A. (2013). Follistatin antagonizes activin signaling and acts with notum to direct planarian head regeneration. *Proc. Natl. Acad. Sci. USA* **110**, 1363–1368.
- Rossi, A., Ross, E.J., Jack, A., and Sánchez Alvarado, A. (2013). Molecular cloning and characterization of SL3: a stem cell-specific SL RNA from the planarian *Schmidtea mediterranea*. *Gene* **533**, 156–167.
- Saló, E., and Baguña, J. (1986). Stimulation of cellular proliferation and differentiation in the intact and regenerating planarian *Dugesia (G) tigrina* by the neuropeptide substance P. *J. Exp. Zool.* **237**, 129–135.
- Salveti, A., Rossi, L., Bonuccelli, L., Lena, A., Pugliesi, C., Rainaldi, G., Evangelista, M., and Gremigni, V. (2009). Adult stem cell plasticity: neoblast repopulation in non-lethally irradiated planarians. *Dev. Biol.* **328**, 305–314.
- Sánchez Alvarado, A., and Newmark, P. (1998). The use of planarians to dissect the molecular basis of metazoan regeneration. *Wound Repair Regen.* **6**, 413–420.
- Sanli, T., Steinberg, G.R., Singh, G., and Tsakiridis, T. (2014). AMP-activated protein kinase (AMPK) beyond metabolism: a novel genomic stress sensor participating in the DNA damage response pathway. *Cancer Biol. Ther.* **15**, 156–169.
- Shi, X., and Garry, D.J. (2006). Muscle stem cells in development, regeneration, and disease. *Genes Dev.* **20**, 1692–1708.
- Suh, Y., Obernier, K., Holz-Wenig, G., Mandl, C., Herrmann, A., Wörner, K., Eckstein, V., and Ciccolini, F. (2009). Interaction between DLX2 and EGFR regulates proliferation and neurogenesis of SVZ precursors. *Mol. Cell Neurosci.* **42**, 308–314.
- Sun, Y., Goderie, S.K., and Temple, S. (2005). Asymmetric distribution of EGFR receptor during mitosis generates diverse CNS progenitor cells. *Neuron* **45**, 873–886.
- Tanaka, E.M., and Reddien, P.W. (2011). The cellular basis for animal regeneration. *Dev. Cell* **21**, 172–185.
- Thi-Kim Vu, H., Rink, J.C., McKinney, S.A., McClain, M., Lakshmanaperumal, N., Alexander, R., and Sánchez Alvarado, A. (2015). Stem cells and fluid flow drive cyst formation in an invertebrate excretory organ. *Elife* **4**, e07405.
- Tu, K.C., Cheng, L.C., Tk Vu, H., Lange, J.J., McKinney, S.A., Seidel, C.W., and Sánchez Alvarado, A. (2015). Egr-5 is a post-mitotic regulator of planarian epidermal differentiation. *Elife* **4**, e10501.
- van Es, J.H., Sato, T., van de Wetering, M., Lyubimova, A., Nee, A.N., Gregorieff, A., Sasaki, N., Zeinstra, L., van den Born, M., Korving, J., et al. (2012). Dll1+ secretory progenitor cells revert to stem cells upon crypt damage. *Nat. Cell Biol.* **14**, 1099–1104.
- van Wolfswinkel, J.C., Wagner, D.E., and Reddien, P.W. (2014). Single-cell analysis reveals functionally distinct classes within the planarian stem cell compartment. *Cell Stem Cell* **15**, 326–339.
- Vaughan, A.E., Brumwell, A.N., Xi, Y., Gotts, J.E., Brownfield, D.G., Treutlein, B., Tan, K., Tan, V., Liu, F.C., Looney, M.R., et al. (2015). Lineage-negative progenitors mobilize to regenerate lung epithelium after major injury. *Nature* **517**, 621–625.
- Vermeulen, L., and Snippert, H.J. (2014). Stem cell dynamics in homeostasis and cancer of the intestine. *Nat. Rev. Cancer* **14**, 468–480.
- Wagner, D.E., Wang, I.E., and Reddien, P.W. (2011). Clonogenic neoblasts are pluripotent adult stem cells that underlie planarian regeneration. *Science* **332**, 811–816.
- Wagner, D.E., Ho, J.J., and Reddien, P.W. (2012). Genetic regulators of a pluripotent adult stem cell system in planarians identified by RNAi and clonal analysis. *Cell Stem Cell* **10**, 299–311.
- Wenemoser, D., and Reddien, P.W. (2010). Planarian regeneration involves distinct stem cell responses to wounds and tissue absence. *Dev. Biol.* **344**, 979–991.
- Witchley, J.N., Mayer, M., Wagner, D.E., Owen, J.H., and Reddien, P.W. (2013). Muscle cells provide instructions for planarian regeneration. *Cell Rep.* **4**, 633–641.
- Wolff, E., and Dubois, F. (1948). Sur la migration des cellules de régénération chez les planaires. *Rev. Suisse Zool.* **55**, 218–227.

Xiang, Y., Miller, D.E., Ross, E.J., Sánchez Alvarado, A., and Hawley, R.S. (2014). Synaptonemal complex extension from clustered telomeres mediates full-length chromosome pairing in *Schmidtea mediterranea*. *Proc. Natl. Acad. Sci. USA* *111*, E5159–E5168.

Yazawa, S., Umesono, Y., Hayashi, T., Tarui, H., and Agata, K. (2009). Planarian Hedgehog/Patched establishes anterior-posterior polarity by regulating Wnt signaling. *Proc. Natl. Acad. Sci. USA* *106*, 22329–22334.

Zhu, S.J., Hallows, S.E., Currie, K.W., Xu, C., and Pearson, B.J. (2015). A *mex3* homolog is required for differentiation during planarian stem cell lineage development. *Elife* *4*, e07025.

Zuo, W., Zhang, T., Wu, D.Z., Guan, S.P., Liew, A.A., Yamamoto, Y., Wang, X., Lim, S.J., Vincent, M., Lessard, M., et al. (2015). p63(+)Krt5(+) distal airway stem cells are essential for lung regeneration. *Nature* *517*, 616–620.